PROCEEDINGS, 41st Workshop on Geothermal Reservoir Engineering
Stanford University, Stanford, California, February 22-24, 2016
SGP-TR-209

Application of Isotopic Approaches for Identifying Hidden Geothermal Systems in Southern Idaho

Mark E. Conrad[1], Patrick F. Dobson[1], Eric L. Sonnenthal[1], B. Mack Kennedy[1], Cody Cannon[2], Wade Worthing[2], Thomas Wood[2], Ghanashyam Neupane[3], Earl Mattson[3] and Travis McLing[3]

[1]Earth and Environmental Sciences Area, Lawrence Berkeley National Laboratory, Berkeley, CA

[2]University of Idaho – Idaho Falls, ID

[3]Idaho National Laboratory, Idaho Fall, ID

Corresponding author: msconrad@lbl.gov

Keywords: Isotopes, geothermometry, Snake River Plain, high-temperature water-rock interaction

ABSTRACT

Southern Idaho is an area of high heat flow with significant potential geothermal resources. However, shallow cold groundwater effectively masks thermal signatures of deep-seated geothermal systems in the area. In order to attempt to see through the shallow groundwater, we are applying a combination of geochemical and isotopic tools relying on dissolved gas and chemical species that have low concentrations in the dilute groundwater to prospect for high-temperature systems in the deep subsurface. For the first phase of the project, our efforts were focused in and around the eastern Snake River Plain (ESRP). We have collected and analyzed the isotopic compositions of more than 40 samples from thermal springs and wells from the region. Of potential isotope geothermometers, the sulfate-water oxygen isotope geothermometer has given the most promising results, yielding calculated temperatures similar to multi-component chemical geothermometers. Other isotopic tools that have proven useful are shifts in the isotopic compositions (δD and $\delta^{18}O$) of groundwater away from the local meteoric water line indicating high-temperature interaction with reservoir rocks or mixing with a magmatically derived fluid. In addition, the δD and $\delta^{13}C$ of dissolved methane in several of the samples indicate that the methane formed in a high temperature magmatic system. Taken together with the analyses of multi-component chemical geothermometry and a separate study of the $^{3}He/^{4}He$ from the same features, the results have identified two promising areas warranting more concentrated study in the Twin Falls area and the Camas Prairie region between the ESRP and the Idaho batholith.

1. INTRODUCTION

The western United States has been identified as an area with high potential for geothermal development (Blackwell et al., 2011) and the eastern Snake River Plain (ESRP) in southern Idaho is one of the most promising regions. The ESRP extends from the Twin Falls area in south-central Idaho northeast to the Yellowstone area (Figure 1). The geology of the ESRP consists of thick deposits of Miocene-Eocene rhyolitic tuff deposits produced from a series of volcanic centers formed by migration of the Yellowstone hotspot to its current location (Pierce and Morgan, 1992; Hughes et al., 1999). The rhyolitic rocks are overlain by Quaternary basalt flows generated from northwest trending volcanic rifts formed from extensional activity following passage of the Yellowstone hotspot (Hughes et al., 1999). The basalt flows and accompanying sedimentary interbeds can reach thicknesses of greater than 1 km. These highly permeable rocks host a major aquifer carrying run-off water from the mountainous regions surrounding the ESRP (Whitehead, 1992).

The high heat flux in the ESRP (~110 mW/m^2; Smith, 2004) and abundant hot springs along the margins of the plain suggest that there should be significant, exploitable geothermal reserves in the area. The deep rhyolitic rocks are the likely host rocks for the geothermal reservoir, with the high heat flow resulting from underlying young basaltic sill intrusions (e.g., Nielson and Shervais, 2014; Welhan, 2015; Shervais et al., 2015), but the high-volume, rapidly flowing shallow aquifer in the overlying basalts makes it difficult to use heat flow measurements to pinpoint areas of high potential. Most water from shallow wells and springs in the ESRP are mixed waters of multiple sources, dominated by meteoric water that may mask or significantly attenuate the thermal signal of any deep geothermal waters (McLing et al., 2002; Welhan, 2015). However, due to the dilute nature of the meteoric water, some of the chemical signatures of the high temperature systems may persist.

We are conducting this study to test the hypothesis that geochemical signatures of deep geothermal activity can be used to "see through" the shallow aquifer in the ESRP. Results of related efforts to compare the results of traditional chemical geothermometry to temperatures calculated using RTEst (Palmer et al., 2014), an advanced multi-component equilibrium geothermometer, are presented elsewhere (Neupane et al., 2016). Briefly, where traditional geothermometry does not account for physical relationships (e.g., boiling, mixing) or chemical equilibrium with complex mineral assemblages typical of real rock systems, RTEst does account for these parameters. In addition, the results of a survey of helium isotope ratios in the samples collected for this project are presented in a previous paper (Dobson et al., 2015). In this paper, the results of isotopic analyses of water (δD and $\delta^{18}O$), dissolved inorganic carbon ($\delta^{13}C$), sulfate ($\delta^{34}S$ and $\delta^{18}O$) and dissolved methane (δD and $\delta^{13}C$) are presented and discussed. The locations of samples collected for this project along with those of previous sampling efforts are plotted on Figure 1 below.

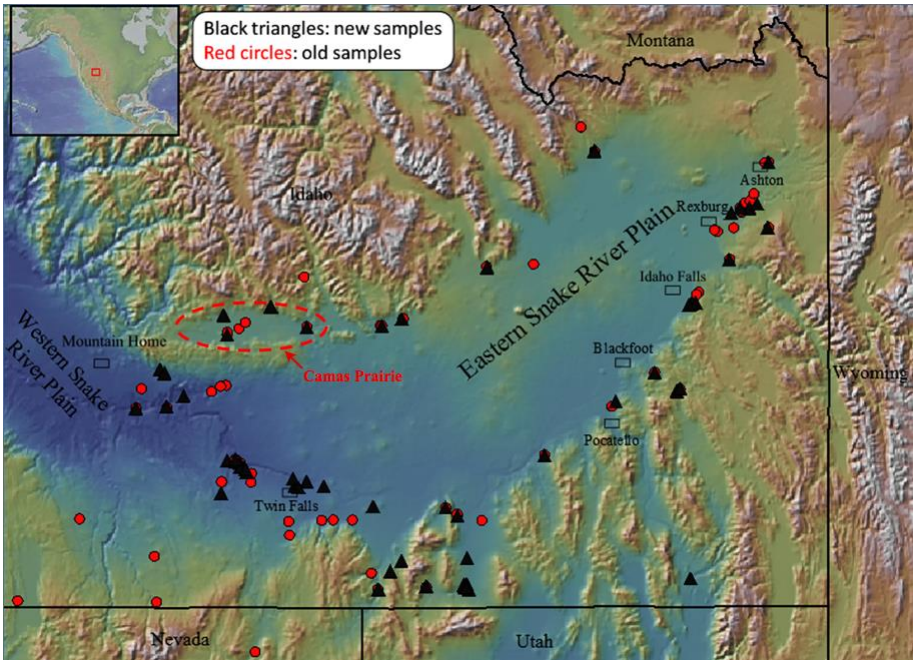

Figure 1: Map of southeastern Idaho showing the Eastern Snake River Plain and the locations of prior geothermal samples plus those collected and analyzed for this project. Note the Camas Prairie area highlighted on the map.

2. FIELD AND LABORATORY METHODS

2.1 Sampling Methods

Samples for this investigation were collected from both groundwater thermal wells and hot springs. Samples from groundwater wells were collected as near the outlet as possible following purging of at least 3 times the volume of water in the well casing. Spring samples were taken as close to the outlet as possible, determined by the hottest point within the features. At each sampling site, 3 types of samples were collected. For δD and $\delta^{18}O$ of water and $\delta^{13}C$ of total dissolved inorganic carbon (DIC), a sample of water was collected directly into a 60 ml syringe rinsed once with water from the source. The sample was then passed through a 0.2 μm filter and injected into a 40 ml amber vial filled to the top and immediately capped. The sample was then stored at 4 °C until it could be analyzed. For analyses of the $\delta^{34}S$ and $\delta^{18}O$ of dissolved sulfate, a 40 ml centrifuge tube was filled with water and HCl added to drop the pH down to ~2 to preserve the sample and drive off any dissolved inorganic carbon in the sample. For dissolved gas samples, filtered water was injected into 60 or 160 ml evacuated vials capped with thick, blue butyl rubber stoppers until the bottle was filled. The sample was stored at 4 °C until it could be analyzed.

2.2 Isotope Analyses

2.2.1 Water Isotope Measurements

The hydrogen and oxygen isotopic compositions of the water samples were analyzed separately at the Center for Stable Isotope Biogeochemistry (CSIB) at the University of California, Berkeley. δD values of water are analyzed using a hot chromium reactor unit (H/Device™) interfaced with a Thermo Delta Plus XL mass spectrometer. The $\delta^{18}O$ in water is analyzed by continuous flow using a Thermo Gas Bench II interfaced to a Thermo Delta Plus XL mass spectrometer. The precision of these analyses determined by repeated analysis of internal standards is ±0.8‰ (1σ) for δD and ±0.12‰ (1σ) for $\delta^{18}O$. Results are presented relative to V-SMOW.

2.2.2 Dissolved Sulfate Isotope Analyses

Following delivery of the acidified samples in the lab, ~1 ml of 1N $BaCl_2$ solution was added to each sample resulting in the precipitation of $BaSO_4$. After waiting >1 day for the precipitates to settle, the supernatant solution is decanted off and de-ionized water added to container and the sample re-suspended. The resulting sample is then centrifuged, the supernatant removed and the sample dried for >1 day. The sulfur and oxygen isotopic composition of the $BaSO_4$ is then analyzed. The sulfur isotope compositions of the samples were analyzed at the Center for Isotope Geochemistry (CIG) at Lawrence Berkeley National Laboratory by combustion in a Costech Elemental Analyzer with the $\delta^{34}S$ values of the resulting SO_2 analyzed on a Thermo Delta V Plus mass spectrometer. The precision of those measurements is ±0.2‰ (1σ). The $\delta^{18}O$ values of the $BaSO_4$ precipitates were analyzed at CSIB using an Elementar PYRO Cube interfaced to a Thermo Delta V mass spectrometer. The precision of those measurements is ±0.5‰ (1σ). Sulfur isotope analyses of H_2S in the samples were also attempted, but the concentrations in the samples were too low.

2.2.3 Dissolved Inorganic Carbon (DIC) Isotope Analyses

The DIC in the samples were analyzed by addition of 0.1 to 1.0 ml of sample to a He-purged vial containing 1 ml of 70% H_3PO_4. The $\delta^{13}C$ values of the resulting CO_2 were then analyzed by injection into a Micromass Trace Gas pre-concentration system interfaced to a

Micromass JA series isotope ratio mass spectrometer at CIG. The precision of those measurements is ±0.3‰ (1σ). Concentrations of DIC in the samples were also determined from these analyses by comparison with standards of known concentrations. These measurements are good to approximately ±10% of the measured value (1σ).

2.2.4 Dissolved Methane Isotopic Analyses

The dissolved gas samples were prepared for analysis by creating a headspace in the sample followed by addition of He gas to the headspace. For isotopic analyses, samples of the headspace gas were flushed through a sample loop on a 6-port Valco Vici valve and then injected into the column of a Thermo Trace Gas Ultra connected to the Delta V Plus mass spectrometer. For $\delta^{13}C$ analyses, the methane was separated chromatographically, and combusted to CO_2, which was then analyzed in the mass spectrometer (1σ precision = ±0.2‰). δD analyses were done by pyrolysing the CH_4 to H_2 gas, which was then analyzed in the mass spectrometer (1σ precision = ±5‰). Concentrations of CH_4 in the headspace were calculated by comparing the total peak areas of the samples to those of known standards. Those concentrations were then converted to dissolved concentrations using Henry's law. Hydrogen isotope analyses of H_2 in the samples were also attempted, but the concentrations were too low.

3. RESULTS AND DISCUSSION

3.1 Sulfate-Water Oxygen Isotope Geothermometer

The difference between the oxygen isotopic compositions of sulfate and water can be used to calculate the temperature of formation of the sulfate (McKenzie and Truesdell, 1977; Fowler et al., 2013). There are, however, several secondary factors that can change the isotopic composition of one or the other of these two phases after the sulfate has formed. For sulfate, mixing with another source of sulfate along the pathway to the surface (e.g., gypsum/anhydrite in evaporite beds) can shift the oxygen isotopic composition of the dissolved sulfate. This can sometimes be inferred based on knowledge of the subsurface geology and/or the sulfur isotope composition of the sulfate. Sulfur in igneous/magmatic systems generally has much lower sulfur isotopic composition than sedimentary gypsum. Microbial reduction of sulfate can also shift the isotopic composition of the residual sulfate, but requires highly anaerobic conditions and will also shift the isotopic composition of the sulfur. The oxygen isotopic composition of the sulfate can also re-equilibrate with the water at lower temperatures, but this is a relatively slow process and is likely only an issue where the thermal waters have a long residence time in a shallower, cooler reservoir. For the water, the biggest issue is mixing with another source of water with a different oxygen isotope composition than the reservoir water. In the ESRP, the isotopic compositions of waters are similar between deep reservoirs and the shallow groundwater. The $\delta^{18}O$ of the water can also be shifted by boiling and/or significant water-rock interaction after formation of the sulfate, but these effects can often be seen by comparison with the hydrogen isotopic composition of the water.

For our temperature calculations, we used the revised sulfate-water oxygen isotope geothermometer formulated by Fowler et al. (2013). To test the applicability of this geothermometer, we collected and analyzed the oxygen isotopic compositions of sulfate and water in fluids injected during a fracture stimulation experiment conducted at the Newberry Volcano in the Oregon Cascades (Cladouhos et al., 2015). About 2.5 million gallons of water were injected under pressure into a subsurface zone at the site and allowed to equilibrate with the rock for 3 weeks. At that point the water was allowed to flow back out of the well and samples were collected for chemical and isotopic analyses. The calculated temperatures using the sulfate-water oxygen isotope geothermometer are plotted on Figure 2 with an average down-hole temperature calculated using GeoT, a multi-component chemical geothermometer (Spycher et al., 2014). The isotope geothermometry values are a bit lower, possibly due to background sulfate, but in general the temperatures appear to be approaching equilibrium for the final samples.

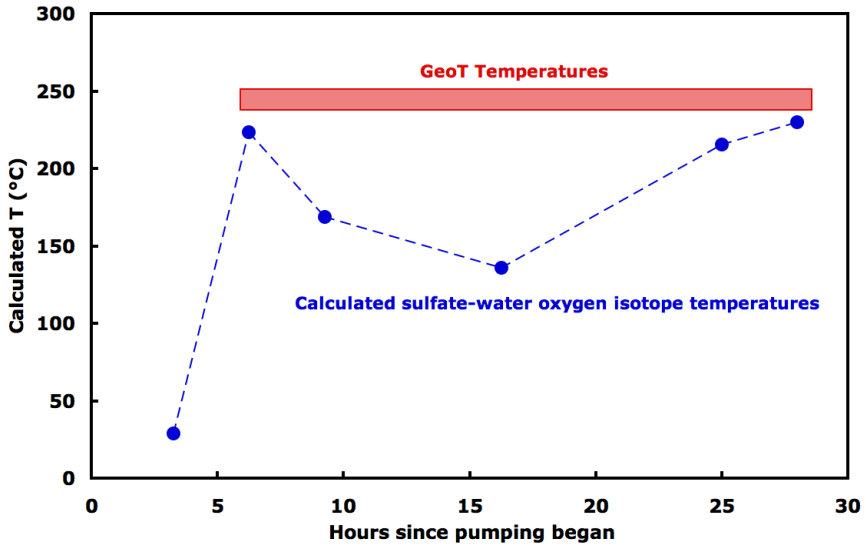

Figure 2: Temperatures calculated for flow-back samples from the Newberry Volcano EGS stimulation test.

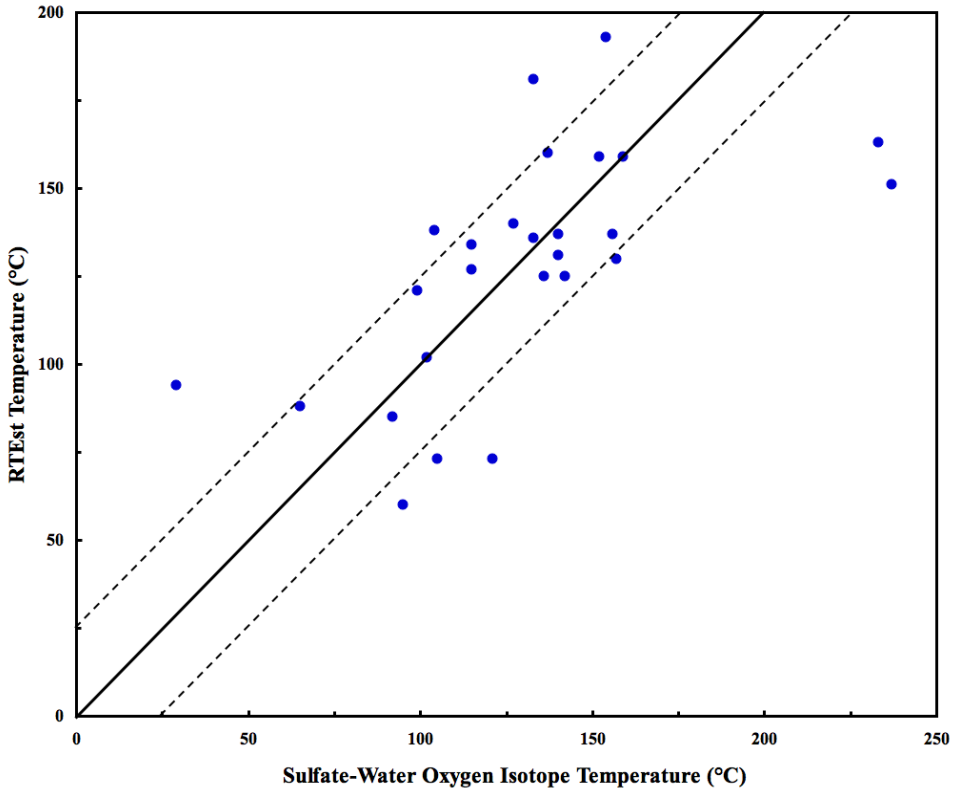

Figure 3: Comparison between temperatures calculated using the sulfate-water oxygen isotope geothermometer versus temperatures calculated using the RTEst. The solid line represents a 1:1 comparison and the dashed lines indicate the range of temperatures within ±25°C of each other.

Temperatures calculated using the sulfate-water oxygen isotope geothermometer for samples collected for this project that contained sufficient sulfate for isotopic analyses are given in Table 1. Also included are RTEst temperatures calculated for the same samples. Given all of the uncertainties associated with both techniques, there is a remarkable correlation between the two geothermometers with most being with ±25°C of each other (Figure 3). In some cases such as Green Canyon Hot Springs and Heise Hot Springs, the sulfate concentrations were high, likely representing interaction with sedimentary evaporite interbeds in the basalts which would result in low calculated temperatures for the sulfate-water oxygen isotope geothermometer. Otherwise, there are no clear explanations for some of the samples with much higher sulfate-water temperatures, suggesting that they might represent deep, hot geothermal systems.

Results calculated with both geothermometers indicate two areas with widespread high temperature geothermal fluids at depth. Temperatures calculated with the sulfate-water oxygen isotope geothermometer for the Twin Falls region average 137°C which is essentially identical to the average temperature calculated with RTEst of 138°C. These values are higher than those reported by Mariner et al. (1997) (90-106°C) for the same region using the sulfate-water oxygen isotope geothermometer. Although these temperatures are on the low side, especially for electricity generation, they come from several features spread across a large area, suggesting there may be hotspots within the region that might be suitable for power generation. The Camas Prairie is the other highly encouraging area with sulfate-water temperatures exceeding 200°C and RTEst temperatures approaching that level. This area was also identified as a geothermal prospect through geothermal play fairway analysis (Shervais et al., 2015).

3.2 Water Isotopes and Water-Rock Interaction

During high-temperature water-rock interaction, the isotopic composition of the water can be shifted to the right of the meteoric water line (Taylor, 1974). The change in the isotopic composition of the water is mostly limited to the oxygen isotopic composition of the water due to the fact that most igneous/volcanic rocks contain very little hydrogen compared to water but have significant oxygen. Mixing with water derived from cooling, degassing magmas can also produce a similar effect (Giggenbach, 1992). Boiling/evaporation will also shift the residual water off the meteoric water line, but these changes will also significantly affect the hydrogen isotopic compositions of the water. It is important to note that mixing with shallower, non-thermal waters can dilute these signals.

The water isotope compositions of the samples collected for this project are plotted on Figure 4. Most of the samples plot close to the meteoric water line (precipitation in this region tends to be slightly offset to the right of the global meteoric water line), but there are several samples that have oxygen isotope composition shifted 1-3‰ to the right of the meteoric water line. Four of these samples collected from three locations are from the Camas Prairie region and are some of those with anomalously high temperatures calculated with the sulfate-water oxygen isotope geothermometer. A water sample associated with a flow zone at 1745 m depth collected from the MH-2 well (which encountered temperatures of 150°C; Nielson and Shervais, 2014) also exhibited a similar shift in its oxygen isotope composition (Freeman, 2013)

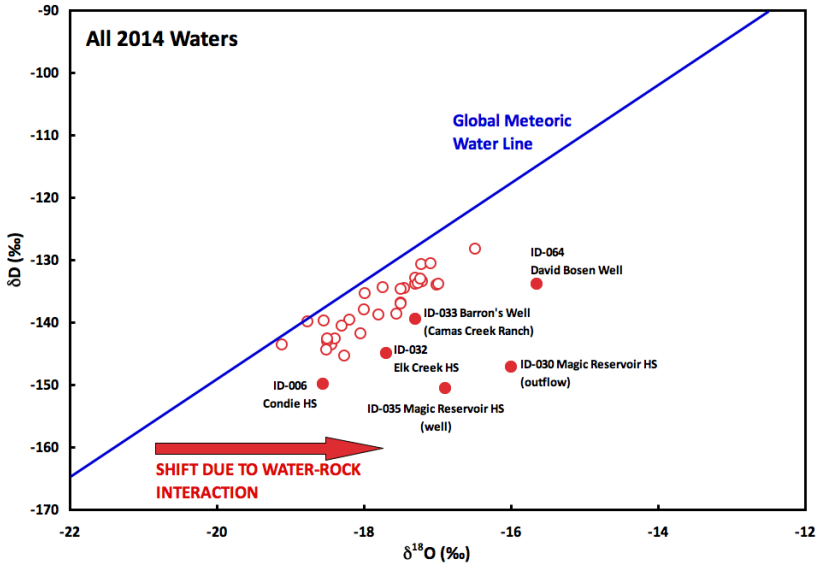

Figure 4: Hydrogen and oxygen isotopic compositions of water from ESRP samples with the global meteoric water line for comparison. Most waters fall very close to the meteoric water line, but there a several that are significantly shifted to the right of the meteoric water line, which is an indication of oxygen isotope exchange during high-temperature water-rock interaction in hydrothermal systems or mixing with magmatically-derived fluids.

3.3 Methane Isotope Signatures of High-Temperature Sources

The carbon and hydrogen isotopic compositions of CH_4 can offer clues as to the mechanism of formation and its post-formation history. Figure 5 is modified from Whiticar et al. (1986) and outlines the primary field of methane formed under thermogenic conditions in hydrocarbon reservoirs and the two primary microbial mechanisms for low-temperature methanogenesis (acetoclastic versus CO_2 reduction). Also shown on this plot is the general field of methane formed abiotically in high-temperature magmatic or hydrothermal systems outlined by Welhan et al. (1988). It is also important to note that the isotopic compositions of the methane can be significantly altered by microbial oxidation in aerobic groundwater.

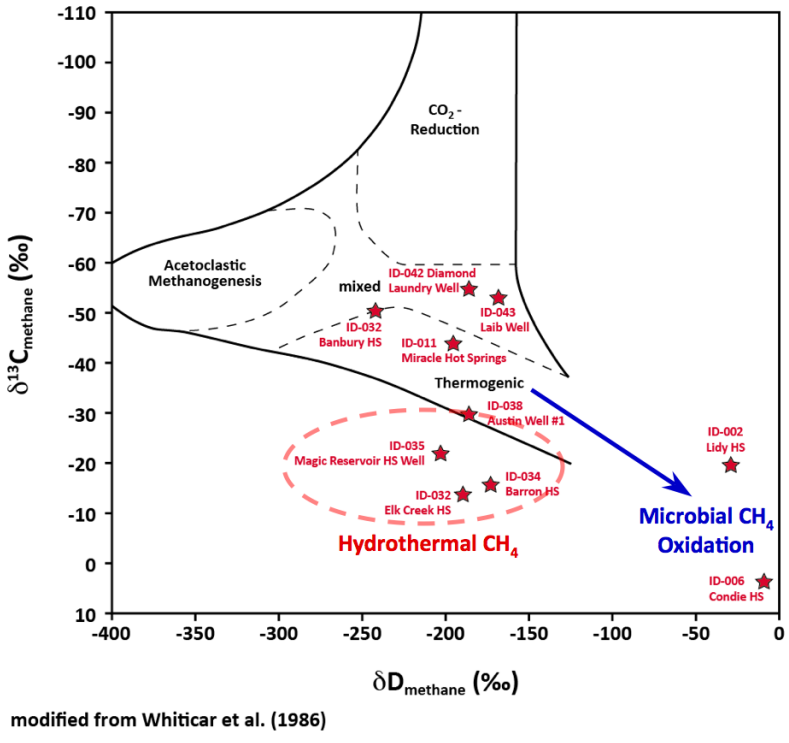

modified from Whiticar et al. (1986)

Figure 5: Carbon and hydrogen isotopic compositions of dissolved methane in samples collected from the ESRP plotted with the ranges of values expected for methane formed by different mechanisms. Most notable are the samples outlined by the red dashed line (all from the Camas Prairie) with isotopic compositions typical of methane formed in high-temperature hydrothermal systems.

The isotopic compositions of samples for which we were able to analyze both the hydrogen and carbon isotopes of CH_4 are plotted on Figure 5. Of this group, there are a couple of samples (Condie Hot Springs and Lidy Hot Springs) that have clearly undergone significant methane oxidation. This is not surprising since both sampling points were from open-air pools of water. The most interesting thing about these samples is that despite significant oxidation, there were still high enough concentrations of methane remaining for isotopic measurements. There are also a number of samples in the thermogenic/mixed origin areas of the plot. These are all from the Twin Falls area and could have been formed from thermal degradation of organic matter in the subsurface. Most interestingly, the remaining 3 samples plot in the field of high temperature hydrothermal methane. These samples are the same three from the Camas Prairie area with the water with the strongly shifted oxygen isotope composition and also have high sulfate-water oxygen isotope temperatures.

4. CONCLUSIONS

The results of study demonstrate the value of isotopic data for identifying areas with high potential for geothermal exploitation, especially when combined with other tools such as multi-component chemical geothermometers. Through this work, we have identified two very promising areas for further study.

1. Numerous intermediate temperature geothermal springs and wells characterize the Twin Falls region. These thermal features yield calculated temperatures in the range of 140±20°C across a wide area and may be indicating the existence of higher temperature hotspots in the region. In addition, helium isotope data collected from some of the same thermal springs and wells (Dobson et al., 2015) indicate the presence of mantle helium that may be related to recent basaltic intrusions that may be providing the heat driving the geothermal activity in the area.

2. Both RTEst and the sulfate-water isotope geothermometer indicate temperatures into the 200°C range at several thermal features in the Camas Prairie. Further, shifts in the isotopic compositions of the thermal waters indicating high-temperature water-rock interaction or mixing with magmatically-derived fluids may be occurring at depth and isotopic signatures of hydrothermal methane also point to significant geothermal resources in the area. Finally, several of these features also had elevated $^3He/^4He$ values indicating the potential presence of a mantle-derived heat source.

ACKNOWLEDGMENTS

This work was conducted with funding from the Assistant Secretary for Energy Efficiency and Renewable Energy, Geothermal Technologies Program, of the U.S. Department under the U.S. Department of Energy Contract Nos. DE-AC02-05CH11231 with Lawrence Berkeley National Laboratory and DE-AC07-05ID14517 with Idaho National Laboratory.

Table 1. Sample data

Location	CAES sample ID	Collection date	Sample Type	Latitude (N)	Longitude (W)	Elevation (m)	Feature type	T (°C)	$\delta^{18}O$ H_2O	δD H_2O
Lidy Hot Springs	002	3/11/14	Water	44.1456	112.5549	1630	outflow	56	-18.2	-140
Green Canyon H.S.	004	3/11/14	Water	43.7918	111.4395	1794	outflow	44	-18.8	-140
Sturm Well	005	3/11/14	Water	44.0932	111.4351	1617	well	31	-18.6	-140
Condie H.S.	006	3/12/14	Water	43.3329	113.9173	1462	hot spring	51	-18.6	-150
Condie H.S.	006	3/12/14	Gas	43.3329	113.9173	1462	hot spring	51		
Green House Well	007	3/12/14	Water	43.6024	113.2422	1621	well	36	-18.4	-144
Eckart Office Well	008	3/13/14	Water	42.6994	114.9104	1039	well	25	-18.3	-145
Campbell Well #1	009	3/13/14	Water	42.6445	114.7830	961	well	35	-17.0	-134
Campbell Well #2	010	3/13/14	Water	42.6450	114.7870	976	well	35	-17.2	-133
Miracle H.S.	011	3/13/14	Water	42.6942	114.8567	893	well	58	-18.0	-142
Driscoll H.S.	013	3/13/14	Water	42.5436	114.9489	1044	hot spring	40	-17.0	-134
CSI campus well #2	014	3/14/14	Water	42.5830	114.4748	1119	well	38	-17.3	-134
Heise Hot Springs	001	6/9/14	Water	43.6428	-111.6877	1527	hot spring		-17.6	-139
RRG1	020	6/11/14	Water	42.1021	-113.3843	1478	Well	150	-17.3	-133
RRG2	021	6/11/14	Water	42.1104	-113.3752	1479	Well	150	-17.5	-134
RRG4	023	6/11/14	Water	42.0979	-113.3854	1479	Well	150	-17.3	-134
Indian Springs	024	6/17/14	Water	42.7259	-112.8738	1374	Thermal	33	-17.2	-131
Grush Dairy	025	6/18/14	Water	42.2367	-113.3697	1418	Well	55		
Milford Sweat H.S.	029	6/23/14	Water	43.3648	113.7888	1520	hot spring	38	-18.3	-141
Magic Reservoir H.S. Outflow	030	6/23/14	Water	43.3278	114.4003	1464	outflow	39	-16.0	-147
Elk Creek H.S.	032	6/23/14	Water	43.4232	114.6286	1733	hot spring	57	-17.7	-145
Barron well	033	6/24/14	Water	43.2924	114.9100	1549	well	38	-17.3	-140
Wardrop HS	034	6/24/14	Water	43.3829	114.9322	1580	hot spring	66	-18.4	-143
Wardrop HS	034	6/24/14	Gas	43.3829	114.9322	1580	hot spring	66		
Magic Reservoir H.S. Well	035	6/24/14	Water	43.3285	114.3997	1472	well	74	-16.9	-151
Magic Reservoir H.S. Well	035	6/24/14	Gas	43.3285	114.3997	1472	well	74		
Prince Albert H.S.	036	6/24/14	Water	43.1297	115.3384	1316	hot spring	58	-18.5	-143
Oakley Warm Spring Well	037	6/25/14	Water	42.1733	113.8616	1619	warm	47	-18.0	-138
Austin Well #1	038	6/25/14	Water	42.0853	113.9398	1469	well	46	-18.5	-143
Marsh Creek Well	039	6/25/14	Water	42.4766	113.5077	1373	well	60	-17.5	-135
Sliger's 1000 Springs Well	040	6/26/14	Water	42.7040	114.8570	892	well	72	-17.8	-139
Banbury Well	041	6/26/14	Water	42.6884	114.8268	894	well	59	-17.5	-137
Banbury H.S.	042	6/26/14	Gas	42.6884	114.8268	894	hot spring	59	-17.5	-137
Diamond Laundry	043	7/16/14	Water	42.9554	-115.3000	783	Well	35	-18.5	-144
Leo Ray Road	046	7/17/14	Water	42.6678	-114.8267	943	Well	36	-17.2	-133
Laib Well	050	7/17/14	Water	42.9463	-115.4942	762	Well	33	-16.5	-128
Durfee H.S.	061	7/24/14	Water	42.1001	-113.6335	1646	Thermal	45	-17.7	-134
Basin Cemetery	062	7/24/14	Water	42.2233	-113.7917	1595	Well	31	-17.1	-131
Wybenga Dairy	063	7/24/14	Water	42.4822	-113.9734	1323	Well	34	-18.0	-135
David Bosen Well	064	7/25/14	Water	42.1394	-111.9371	1444	Well	90	-15.7	-134

Table 1 (continued). Sample data

Location	$\delta^{34}S_{SO4}$ (‰)	$\delta^{18}O\ SO_4$	$\Delta^{18}O_{SO4\text{-}H2O}$	T_{SO4} (°C)	RTEst T (°C)	DIC (mM)	$\delta^{13}C_{DIC}$ (‰)	Dissolved CH_4 (nM)	Gas CH_4 (ppm)	$\delta^{13}C_{CH4}$ (‰)	δD_{CH4} (‰)
Lidy Hot Springs	3.8	-3.4	14.8	127	140	5.4	-1.5	2.6		-19.7	-29
Green Canyon H.S.	22.6	11.6	30.3	29	94	4.2	-2.8	0.4		-16.1	
Sturm Well					152	1.6	-11.6				
Condie H.S.	18.2	-0.9	17.6	102	91	9.9	-2.1	1.4		3.6	-9
Condie H.S.									1282	3.7	27
Green House Well	14.4	0.1	18.6	95	60	9.4	-3.5				
Eckart Office Well	5.5	-2.2	16.1	115	127	1.9	-3.1				
Campbell Well #1	6.2	-3.4	13.6	140	137	3.7	-7.5				
Campbell Well #2	6.3	-3.6	13.6	140	131	3.7	-7.2				
Miracle H.S.	6.6	-4.2	13.8	137	160	1.5	-4.6	2.2		-44.0	-195
Driscoll H.S.	5.7	-4.8	12.2	156	137	2.9	-11.2				
CSI campus well #2	6.6	-3.0	14.3	133	136	2.6	-7.2				
Heise Hot Springs	20.3	5.4	23.0	65	88	21.4	3.7				
RRG1	13.9	-9.0	8.3	214	162	1.2	-5.4	0.6		-49.1	
RRG2	13.2	1.5	19.0	92	148	0.7	-5.0	0.9		-55.5	
RRG4	14.6	-9.6	7.7	224	139	0.9	-2.6				
Indian Springs	5.2	-6.4	10.8	174	70	2.0	-4.4				
Grush Dairy					102	1.6	-2.2				
Milford Sweat H.S.	15.8	-1.0	17.3	105	73	3.2	-1.6	1.6		-55.5	
Magic Reservoir H.S. Outflow	21.6	-8.7	7.3	233	163						
Elk Creek H.S.	13.1	-3.7	14.0	136	125	1.4	-4.2	6.8		-13.8	-189
Barron well	-8.3	-15.9	1.4	419	79	2.1	-6.9	2.6		-48.9	
Wardrop HS	7.0	-4.2	14.2	133	181	1.0	-7.0	2.8		-12.8	
Wardrop HS									2016	-15.8	-173
Magic Reservoir H.S. Well	21.9	-9.8	7.1	237	151	13.1	-0.9				
Magic Reservoir H.S. Well									3160	-22.0	-203
Prince Albert H.S.	8.3	-6.1	12.4	154	193	0.9	-8.6	0.5		-23.7	
Oakley Warm Spring Well	13.4	-5.9	12.1	157	130						
Austin Well #1	14.8	0.4	18.9	92	85	1.5	-2.7	12.9		-29.8	-186
Marsh Creek Well	10.2	-4.1	13.4	142	125	1.7	-4.4	2.4		-31.5	
Sliger's 1000 Springs Well	11.6	-1.7	16.1	115	134	1.2	-4.2	2.2		-47.6	
Banbury Well	6.0	-5.6	11.9	159	159	1.9	-5.9	1.7		-51.3	
Banbury H.S.	4.7	-5.0	12.5	152	159				2140	-50.5	-242
Diamond Laundry					70					-54.9	
Leo Ray Road		0.8	18.0	99	121						
Laib Well					83					-53.1	
Durfee H.S.		-0.4	17.4	104	138						
Basin Cemetery		-1.6	15.5	121	73						
Wybenga Dairy					132						
David Bosen Well					175					-37.8	

REFERENCES

Blackwell, D.D., M.C. Richards, Z.S. Frone, J.F. Batir, M.A. Williams, A.A. Ruzo, R.K Dingwall (2011), SMU Geothermal Laboratory Heat Flow Map of the Conterminous United States, 2011: Available at http://www.smu.edu/geothermal.

Cladouhos, T.T., Petty, S., Swyer, M.W., Uddenberg, M.E., Grasso, K., and Nordin, Y.: Results from Newberry Volcano EGS Demonstration, 2010–2014. Geothermics (2015), http://dx.doi.org/10.1016/j.geothermics.2015.08.009.

Dobson, P.F., B.M. Kennedy, M.E. Conrad, T. McLing, E. Mattson, T. Wood, C. Cannon, R. Spackman, M. van Soest and M. Robertson (2015) He Isotopic Evidence for Undiscovered Geothermal Systems in the Snake River Plain, *Proceedings*, Fortieth Workshop on Geothermal Reservoir Engineering, Stanford University, Stanford, California, January 26-28, 2015.

Freeman, T.G. (2013) Evaluation of the geothermal potential of the Snake River Plain, Idaho, based on three exploration holes. MS thesis, Utah State University, 90 p.

Fowler, A.P.G, L.B. Hackett, C.W. Klein (2013) Reformulation and performance evaluation of the sulfate-water oxygen isotope geothermometer: *CRC Transactions* **37**, 393-401.

Giggenbach, W.F. (1992) Isotopic shifts in waters from geothermal and volcanic systems along convergent plate boundaries and their origins. *Earth and Planetary Science Letters* **113**, 495-510.

Hughes, S.S., Smith, R.P., Hackett, W.R., and Anderson, S. R.: Mafic volcanism and environmental geology of the eastern Snake River Plain. *Idaho Guidebook to the Geology of Eastern Idaho*. Idaho Museum of Natural History, (1999), 143-168.

Mariner, R.H., Young, H.W., Bullen, T.D., and Janik, C.J.: Sulfate-water isotope geothermometry and lead isotope data for the regional geothermal system in the Twin Falls area, south-central Idaho. *Geothermal Resources Council Transactions* **21**, (1997), 197-201.

McLing, T.L., Smith, R.W., and Johnson, T.M.: Chemical characteristics of thermal water beneath the eastern Snake River Plain. In: Geology, Hydrogeology, and Environmental Remediation: Idaho National Engineering and Environmental Laboratory, Eastern Snake River Plain, Idaho, P.K. Link and L.L. Mink, eds. *Geological Society of America Special Paper* **353**, (2002), 205-211.

McKenzie, W.F., and Truesdell, A.H.: Geothermal reservoir temperatures estimated from the oxygen isotope compositions of dissolved sulfate and water from hot springs and shallow drillholes. *Geothermics* **5**, 51-61.

Neupane, G., Mattson, E.D., Cannon, J.C., Atkinson, T.A., McLing, T.L., Wood, T.R., Dobson, P.F., and Conrad, M.E.: Potential hydrothermal resource areas and their reservoir temperatures in the Eastern Snake River Plain, Idaho. *Proceedings*, 41st Workshop on Geothermal Reservoir Engineering, Stanford University, Stanford, California, February 22-24, 2016 SGP-TR-209 (2016).

Nielson, D.L., and Shervais, J.W. (2014) Conceptual model for Snake River Plain geothermal systems, *Proceedings*, 39th Workshop on Geothermal Reservoir Engineering, Stanford University, Stanford, CA, SGP-TR-202.

Palmer, C.D., Ohly, S.R., Smith, R.W., Neupane, G., McLing, T., Mattson, E.: Mineral selection for multicomponent equilibrium geothermometry. *GRC Transactions*, **38**, (2014), 453-459.

Pierce, K. L., and Morgan, L. A.: The track of the Yellowstone hot spot: Volcanism, faulting, and uplift. *Geological Society of America Memoirs*, **179**, (192), 1-54.

Shervais, J.W., Glen, J.M., Liberty, L.M., Dobson, P., Gasperikova, E., Sonnenthal, E., Visser, C., Nielson, D., Garg, S., Evans, J.P., Siler, D., DeAngelo, J., Athens, N., and Burns, E. (2015) Snake River Plain Play Fairway Analysis – Phase I report. Geothermal Resources Council Transactions 39, 761-769.

Smith, R.P.: Geologic setting of the Snake River Plain aquifer and vadose zone. *Vadose Zone Journal*, **3**, (2004), 47-58.

Spycher, N., Peiffer, L., Saldi, G., Sonnenthal, E., Reed, M.H., and Kennedy, B.M. (2014) Integrated multicomponent solute geothermometry. *Geothermics* **51**, 113–123.

Taylor, H.P. (1974) Application of oxygen and hydrogen isotope studies to problems of hydrothermal alteration and ore deposition. *Econ. Geol.* **69**, 843-883.

Welhan, J.A. (2015) Thermal and trace-element anomalies in the Eastern Snake River Plain aquifer: Towards a conceptual model of the EGS resource. *GRC Transactions* **39**, 363-376.

Welhan, J.A., R.J. Poreda, W. Rison, H. Craig (1988) Helium isotopes in geothermal and volcanic gases of the western United States: I. Regional variability and magmatic origin: *J. Volcanology Geotherm. Res.* **34**, 185–199.

Whitehead, R.L.: Geohydrologic framework of the Snake River Plain regional aquifer system, Idaho and eastern Oregon. Regional aquifer system analysis-Snake River Plain, Idaho. *US Geological Survey Professional Paper 1408-B*, (1992).

Whiticar, M.J., E. Faber and M. Schoell (1986) Biogenic methane formation in marine and fresh-water environments – CO_2 reduction versus acetate fermentation isotope evidence. *Geochim. Cosmochim. Acta* **50**, 693-709.